DTU Library

The effect of hydrogen bonding on torsional dynamics: A combined far-infrared jet and matrix isolation study of methanol dimer.

Kollipost, F.; Andersen, Jonas; Wallin Mahler Andersen, Denise; Heimdal, J.; Heger, M.; Suhm, M. A.; Larsen, René Wugt

Link back to DTU Orbit

The effect of hydrogen bonding on torsional dynamics: A combined far-infrared jet and matrix isolation study of methanol dimer

F. Kollipost, J. Andersen, D. W. Mahler, J. Heimdal, M. Heger, M. A. Suhm, and R. Wugt Larsen

The effect of hydrogen bonding on torsional dynamics: A combined far-infrared jet and matrix isolation study of methanol dimer

F. Kollipost,[1] J. Andersen,[2] D. W. Mahler,[2] J. Heimdal,[3] M. Heger,[1] M. A. Suhm,[1] and R. Wugt Larsen[2,a)]

[1]*Institut für Physikalische Chemie, Universität Göttingen, Tammannstr. 6, D-37077 Göttingen, Germany*
[2]*Department of Chemistry, Technical University of Denmark, Kemitorvet 206, DK-2800 Kgs. Lyngby, Denmark*
[3]*MAX-IV Laboratory, Lund University, P. O. Box 118, SE-22100 Lund, Sweden*

The effect of strong intermolecular hydrogen bonding on torsional degrees of freedom is investigated by far-infrared absorption spectroscopy for different methanol dimer isotopologues isolated in supersonic jet expansions or embedded in inert neon matrices at low temperatures. For the vacuum-isolated and Ne-embedded methanol dimer, the hydrogen bond OH librational mode of the donor subunit is finally observed at ∼560 cm^{-1}, blue-shifted by more than 300 cm^{-1} relative to the OH torsional fundamental of the free methanol monomer. The OH torsional mode of the acceptor embedded in neon is observed at ∼286 cm^{-1}. The experimental findings are held against harmonic predictions from local coupled-cluster methods with single and double excitations and a perturbative treatment of triple excitations [LCCSD(T)] and anharmonic. VPT2 corrections at canonical MP2 and density functional theory (DFT) levels in order to quantify the contribution of vibrational anharmonicity for this important class of intermolecular hydrogen bond vibrational motion. © *2014 AIP Publishing LLC*. [http://dx.doi.org/10.1063/1.4900922]

I. INTRODUCTION

Methanol is one of the most important flexible molecules for the study of internal rotation or torsional motion, a class of large-amplitude vibrational motion in which two parts of the same molecule rotate with respect to each other over distances comparable to chemical bond lengths. In the case of methanol, the methyl group can counter-rotate with respect to the hydroxy group around the C–O bond axis. The coupling between large-amplitude torsional motion and other vibrational motions of a molecule is known to accelerate the transfer of energy internally among the vibrational modes via intramolecular vibrational redistribution (IVR).[1,2] These energy transfer processes are particularly important in order to understand the quantum control of chemical reactions via laser-induced bond breaking by torsion-mediated IVR relaxation in molecules containing a methyl rotor.[3] More generally, the torsional degrees of freedom are of critical importance in the development of molecular force fields for flexible molecules.[4]

In cyclic methanol clusters, the torsional motion of all the subunits is affected significantly by intermolecular hydrogen bonding, and the resulting hydrogen bond librational motion is effectively decoupled from the methyl group rotation.[5,6] The librational motion should not be described as torsional or rotational, but more or less as a genuine localized displacement of the hydrogen-bonded H atoms. As such, this displacement probes a substantial range of the anharmonic hydrogen bond potential and may be regarded as one of the most sensitive markers of hydrogen bonding. The role of librational motion in intermolecular energy transfer processes of condensed

phases is currently being discussed.[7] Recent quantum chemical studies of the methanol dimer (Fig. 1) show that the incorporation of the donor OH librational mode is essential in order to capture the physics of the predissociation pathway that follows OH stretching excitation[8] since it has been shown to effectively absorb the initially deposited energy. This fits the results from ultra-fast pump-probe experiments of the hydrogen bond breaking dynamics.[9]

The spectroscopy of the hydrogen-bonded methanol dimer has been studied intensely. The rotational spectrum of several methanol dimer isotopologues isolated in molecular beams has been obtained by Lovas *et al.* and its analysis showed that the methanol dimer exhibits a linear hydrogen bond.[10,11] The first experimental study of methanol dimer was reported by Hoffbauer *et al.* who investigated the infrared photodissociation spectrum in the CO stretching region.[12] The observation and assignment of one single C–O stretching band was updated by Huisken and Stemmler who observed two well-separated bands in this region at 1026.5 and 1051.6 cm^{-1}.[13] This observation has been confirmed by subsequent experimental works and supported by theoretical studies.[14–16] The red-shifted dimer band has been assigned to the free CO stretching mode of the acceptor subunit whereas the latter more intense and blue-shifted band has been assigned to the CO stretching mode of the more perturbed H-atom donor molecule. The red-shift originates from an elongation of the acceptor C–O bond distance in the attractive hydrogen bond and the blue-shift results from a stronger force constant and coupling to the OH stretching mode which compresses the C–O bond distance.[17]

A particularly sensitive probe for the hydrogen bond interaction in methanol dimer is the OH stretching mode of the donor subunit. A significant elongation of its O–H

---

a)Author to whom correspondence should be addressed. Electronic mail: rewl@kemi.dtu.dk
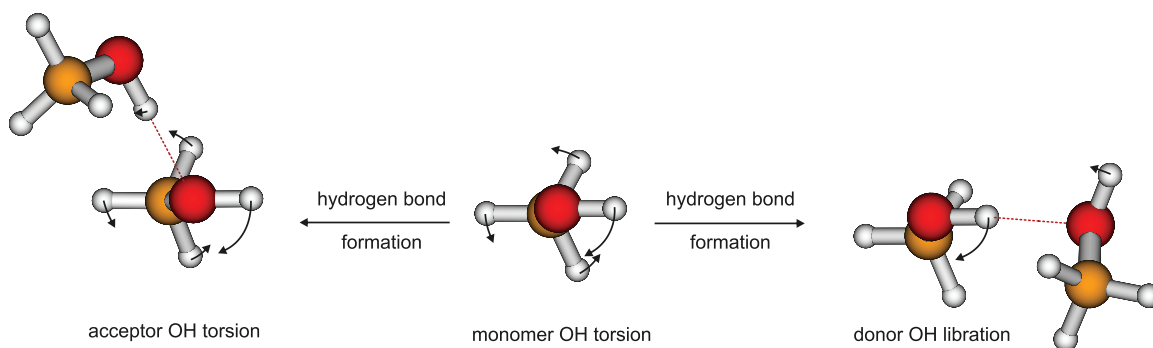
FIG. 1. The normal mode description of the acceptor OH torsional mode and the hydrogen-bonded donor OH librational mode of the methanol dimer.

bond distance upon hydrogen bonding together with a significantly increased OH transition dipole moment provides both a pronounced red-shift and infrared band intensity gain of this chromophore. A variety of independent experimental approaches – infrared photodissociation,[18] cavity ring-down,[19] IR-UV photoionization,[20] spontaneous Raman and direct absorption FTIR spectroscopies[21,22] in supersonic jet expansions – have settled the band origin at around 3575 cm^{-1} with a red-shift of ∼111 cm^{-1} from the monomer band origin, although slight ambiguities exist in the interpretation of the exact monomer reference due to its complicated band structure. Recently, this red-shift has been decomposed into a harmonic contribution[23] of about 121 cm^{-1} and a diagonal anharmonicity correction of 26 cm^{-1},[24] leaving only about −36 cm^{-1} for the combined coupling of all other modes to the hydrogen-bonded OH stretching vibration. The free OH stretching mode of the acceptor subunit has been located around 3684 cm^{-1}[17] and also somewhat lower in wavenumber[20] but in any case close to the monomer band origin.

The most valuable among the technologically accessible spectroscopic observables for the intermolecular potential energy landscape spanned by two interacting methanol molecules is the donor OH librational mode induced by the hydrogen bond. The observation and assignment of this large-amplitude mode provides direct benchmarks for theoretical descriptions of anisotropy and anharmonicity for the hydrogen bond. To the best of our knowledge, the only attempts to explore this crucial observable in the challenging far-infrared region of the electromagnetic spectrum have employed the medium of cryogenic matrices of nitrogen, argon, and carbon monoxide.[25–28] These matrix hosts are known to cause significant matrix-induced perturbations and potential site effects. In nitrogen matrices, up to four different isomers or differently trapped species have been reported with donor OH librational band origins between 572 and 624 cm^{-1} and perturbed acceptor OH torsional band origins between 325 and 386 cm^{-1} relative to the monomer OH torsional band at 304 cm^{-1}.[25] In the present work, we are revisiting these far-infrared spectral signatures of methanol dimer by detecting them in supersonic jet expansions and in less perturbative cryogenic neon matrices.

To discuss the anharmonicity of and the cross-talk between the different vibrational modes, we make use of the simple second-order perturbation theory relationship[29–31] between anharmonic fundamental transitions $\tilde{\nu}_i$ and harmonic normal modes ω_i in the presence of all other modes j

$$\tilde{\nu}_i = \omega_i + 2x_{ii} + \frac{1}{2}\sum_j x_{ij}, \qquad (1)$$

where x_{ii} and x_{ij} are diagonal and off-diagonal anharmonicity constants, respectively. While the former can be easily extracted from overtone transitions, the latter are obtainable from combination bands. Neither of these are accessible in the present experimental work for the methanol dimer OH librational modes, but we can still draw important conclusions from benchmark calculations in the recent literature,[23,24] which have been made available to us by the authors and are mostly contained in the corresponding electronic supplements.

II. EXPERIMENTAL DETAILS

The infrared absorption spectra of jet-cooled methanol clusters were obtained by the high-throughput FTIR jet apparatus at Universität Göttingen described in detail elsewhere.[32] Helium gas pulses on the order of 0.5 mol doped with traces of CH$_3$OH (99.9% atom, VWR) were expanded through a 600 mm long and 0.2 mm wide pulsed slit nozzle into a 23 m^3 vacuum buffer dilution volume. The resulting supersonic jet expansions were synchronously probed by single 2–4 cm^{-1} resolution scans of a rapid-scan Bruker IFS 66v/S FTIR spectrometer. The buffer dilution volume was continuously evacuated by a series of Roots blowers at a pump speed of 2500 m^3 h^{-1} with time intervals of ∼50 s between the pulses to prevent any Mach disk interference by shock waves. The stagnation pressure in the gas reservoir from which the pulsed expansions emerge was 0.8 bar with sample concentrations in the range of 0.3%–0.8%. The mid-infrared spectra were obtained employing a conventional globar radiation source combined with CaF$_2$ beamsplitter and optics and a liquid nitrogen cooled InSb detector. The far-infrared spectra (190–650 cm^{-1}) were recorded employing a 6 μm multilayer Mylar beam splitter, CsI optics, and a liquid-helium cooled Si bolometer from Infrared Labs, Inc. Scans of approximately 400 pulses were collected and averaged for each sample concentration.

For the matrix isolation experiments, neon gas (L'Air Liquide, 99.996%) was deposited via a liquid nitrogen pre-cooled inlet tube with a flow rate of 0.02 mol/h at 3.6 K on a
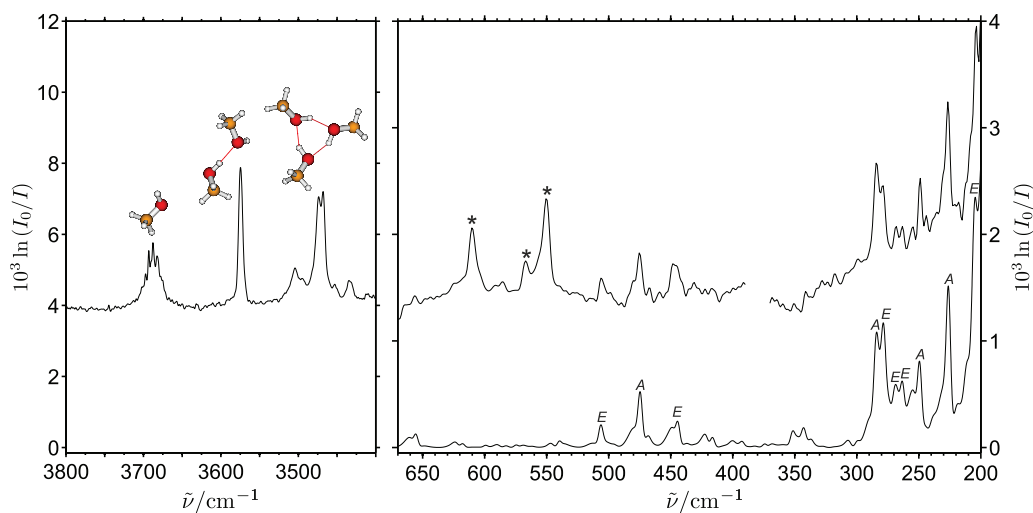
FIG. 2. The combined mid-infrared OH-stretching (upper left trace) and far-infrared (upper right trace) absorption spectrum recorded for supersonic jet expansions of helium doped with methanol together with a simulated rovibrational far-infrared spectrum of methanol monomer based on observations reported in Ref. 42 (lower trace, T_{rot} = 25 K). The methanol cluster bands observed in the far-infrared region are marked with asterisks whereas the Q-branches of the torsional fundamental of methanol monomer are labeled by the symmetry species.

gold-plated oxygen-free high thermal conductivity (OFHC) copper mirror inside an immersion helium cryostat (IHC-3) modified for matrix isolation spectroscopy[33] at MAX-lab. Degassed samples of CH_3OH (Sigma-Aldrich, 99.9% atom) or CH_3OD (Sigma-Aldrich, 98%) were deposited simultaneously with the matrix gas by a separate inlet tube, giving mixing ratios of $\simeq 0.5$–5 permille. The sample temperature at the mirror was monitored by a Lake Shore silicon diode and was kept stable at 2.8 ± 0.1 K before and after the matrix deposition employing resistive heaters and feedback electronics. In most cases, the doped neon matrices were afterwards annealed up to 9 K for the study of temperature effects. The sample mount was equipped with interchangeable CsI and TPX windows, and combined mid-infrared and THz single-beam spectra were collected by a Bruker IFS 120 FTIR spectrometer employing a globar lamp as radiation source. Broadband HgCdTe and InSb detectors combined with a Ge/KBr beam splitter and a Si-bolometer operating at 4.2 K combined with a 6 μm multilayer Mylar beam splitter were employed for the IR and THz spectral regions, respectively. A spectral resolution between 0.1 and 1 cm^{-1} was applied depending on the observed band widths.

III. METHANOL ISOLATED IN SUPERSONIC JET EXPANSIONS

The OH stretching region helps to monitor the size distribution of clusters in the supersonic jet expansions[19,21,22] (see Fig. 2, upper left trace). A reported band origin of 3681.5 cm^{-1} for the monomer OH stretching band based on the center of gas-phase Q-branches[34,35] has been employed in a range of cluster studies.[19,21,35–38] A band origin at 3686 cm^{-1} has subsequently been established by complementary Raman and infrared studies of jet-cooled methanol.[22,39] This value corresponds to the high-frequency component of the jet-Raman spectrum[39] and the absorption maximum in the jet-

FTIR spectrum[22] and agrees well with the band origin of 3685 cm^{-1} obtained from a high-resolution rovibrational analysis of this strongly coupled torsion-vibration system.[40] In addition, the spacing of $\sim$2.6 cm^{-1} between the two observed Q-branches in the jet-Raman spectrum[39] agrees perfectly with the difference in tunneling splitting between the vibrational ground state and the excited OH stretching state.[41] The red-shifted donor OH stretching band origin of 3575 cm^{-1} for the methanol dimer has been established by complementary jet-cooled Raman and FTIR observations whereas the free acceptor OH stretching band overlaps with the rotational structures and torsional tunneling splittings of the monomer band.[21,22] The complicated OH stretching jet spectrum of the cyclic methanol trimer has been shown to involve a vibrational Franck-Condon effect[22] and consists of two near-degenerate strong bands at 3469 cm^{-1} and 3474 cm^{-1}. These two strong bands are accompanied by five weaker sub-bands and no hydrogen-bond isomerism of methanol trimer has to be invoked to understand these jet spectral features.

The upper right trace in Fig. 2 shows the far-infrared absorption spectrum of jet-cooled methanol down to the CsI cut-off close to 200 cm^{-1}. In the region around 370 cm^{-1}, the 6 μm multilayer Mylar beam splitter has a strong dip in the throughput and thereby causes an artifact in the generated absorption spectrum. In the lower far-infrared region, the absorption spectrum reproduces a very rich structure caused by multiple rovibrational sub-bands associated with the torsional fundamental band of the methanol monomer. The large-amplitude torsional motion of methanol is coupled to the overall rotational motion and the other vibrational modes of the molecule. The analysis of these couplings have been described in detail elsewhere.[43] The lower right trace of Fig. 2 shows a rovibrational simulation based on previously assigned Q-branch structures reported in the methanol atlas of Moruzzi *et al.*[42] The room temperature (T_1) spectra were converted to spectra at cold temperatures T_2 by the following

relationship:

$$\frac{S_{nm}(T_1)}{S_{nm}(T_2)} = \frac{e^{-\frac{E_m}{kT_1}}\left(1 - e^{-\frac{hc\tilde{v}_{nm}}{kT_1}}\right)}{e^{-\frac{E_m}{kT_2}}\left(1 - e^{-\frac{hc\tilde{v}_{nm}}{kT_2}}\right)} \qquad (2)$$

employing the line strength S_{nm} and wavenumber $\tilde{v}_{nm}$ of a transition from a lower state m to an upper state n and the energy E_m of the m level. The simulated far-infrared spectrum in Fig. 2 is plotted as an overlay of Gaussian curves with 4 cm^{-1} full widths at half maximum matching the spectral resolution of the jet experiment. It was found that a simulated spectrum at $T_2 = 25$ K yields the best match with the experimental jet spectra. Non-equilibrium effects in the jet expansion concerning the population of the A and E states[44] were ignored, because these are not significant at 25 K.

The most distinct spectral features observed in the lower far-infrared absorption spectrum are located around 205 cm^{-1}, 226 cm^{-1}, 278 cm^{-1}, and 284 cm^{-1} with decreasing intensity for the transitions at higher wavenumbers. These have previously been attributed to Q-branches of different A–A (226 and 284 cm^{-1}) and E–E (205 and 278 cm^{-1}) sub-bands with $\Delta K = \pm 1$ and $K'' \leq 1$ associated with the torsional fundamental.[42] Another observed series of distinct spectral features has previously been attributed to other, less intense A–A (249 cm^{-1}) and E–E (263 and 269 cm^{-1}) torsional sub-bands with $\Delta K = \pm 1$ and $K'' \leq 2$.[42] The convincing agreement between the observed jet spectra and the simulated rovibrational spectrum of the monomer in the low far-infrared spectral region does not at first sight point at any potential methanol dimer contributions.

In the upper far-infrared region above the beam splitter artifact, another three distinct spectral features are reproduced with band origins around 448 cm^{-1}, 475 cm^{-1}, and 507 cm^{-1}. These spectral features can be assigned to three different sub-bands or Q-branches associated with the first torsional overtone of the methanol monomer which are included in the simulated rovibrational spectrum shown in Fig. 2. The Q-branches observed around 448 and 507 cm^{-1} have previously been assigned to the E–E transitions corresponding to $K = -1 \rightarrow -2$ and $K = -1 \rightarrow 0$, respectively, whereas the Q-branch observed around 475 cm^{-1} has previously been assigned to the A–A transition corresponding to $K = 0 \rightarrow +1$.[42] The simulated rovibrational spectrum shown in Fig. 2 includes a total of 17 previously assigned sub-bands with $K'' \leq 3$ associated with the first torsional overtone of methanol in the range from 343 cm^{-1} to 656 cm^{-1}. None of the 14 weaker torsional overtone Q-branches of the monomer are observed clearly in the present far-infrared jet-spectra. The strong spectral features observed in the range from 520 cm^{-1} to 650 cm^{-1} must therefore be assigned to jet-cooled clusters of methanol.

The mid-infrared OH stretching spectral signatures have previously guided the assignment of a number of hydrogen-bonded OH librational modes of jet-cooled methanol trimers and tetramers in the upper far-infrared region.[6, 22] Assisted by dedicated concentration-dependence spectral series, direct comparisons with the corresponding OH stretching spectra

and quantum-chemical predictions, we have previously assigned the observed band at 613 cm^{-1} to the most IR-active OH librational mode of the methanol trimer (see Fig. 2, upper right trace).[5] In addition, two bands have been assigned to the librational modes of the cyclic methanol tetramer: a highly IR-active doubly degenerate mode at 760 cm^{-1}, and a lower-wavenumber mode at 695 cm^{-1} with lower infrared activity (not shown).[5] Subsequently, an upgraded configuration of the experimental jet-FTIR apparatus including a liquid helium cooled Si-bolometer detector revealed the existence of a band centered around 551 cm^{-1} which we tentatively assigned to the lowest-wavenumber OH librational mode of the cyclic trimer,[6] although quantum-chemical calculations have predicted an overlap with the donor OH librational band of the methanol dimer[5] and the relative intensity is indeed higher than predicted. In the present work, featuring an improved signal-to-noise performance in the lower far-infrared region,[45] the existence of the 551 cm^{-1} band is easily confirmed with a reproducible high-wavenumber shoulder at 567 cm^{-1} and an overall higher intensity than the 613 cm^{-1} band as seen in Fig. 2. However, a completely unambiguous size assignment of the 551 cm^{-1} band cannot be obtained by dedicated jet experiments from the concentration dependency alone. Trimer formation cannot be effectively suppressed once dimer formation is favored in the earlier stages of the expansions, and extreme dilutions are not compatible with signal-to-noise limitations in this spectral region. A dimer OH librational fundamental below 551 cm^{-1} or above 567 cm^{-1} can be safely ruled out from the jet experiments, but there could be one or more spectral features attributed to this band in this interval. Therefore, we consult a more sensitive matrix isolation approach where the discrimination between dimer and trimer spectral fingerprints is easier.

IV. METHANOL EMBEDDED IN NEON MATRICES

In previous studies of methanol embedded in solid matrices of para-H$_2$[46] and neon,[47,48] these inert matrix environments have been shown to completely forbid the overall rotational motion of methanol but still allow for large-amplitude internal torsional motion which is just slightly hindered relative to the gas phase. The torsion-vibration splittings into A and E sub-levels by torsional tunneling therefore persist in the inert neon matrix environment, but their standard A–A and E–E selection rules have been shown not to apply anymore.[47] The torsional fundamental of the methanol monomer accordingly gives rise to four different sub-bands (see Fig. 3). In cryogenic neon matrices, the splitting of the ground state of the torsional vibration is reduced from the gas phase value of 9.1 cm^{-1} to 6.7 cm^{-1}, whereas the splitting of the first excited state is reduced from the gas phase value of 86.5 cm^{-1} to 56.2 cm^{-1}.[47] Both of these vibrational splittings can be revealed by dedicated annealing experiments. Fig. 3 shows the observed far-infrared absorption spectrum of methanol embedded in neon at 2.8 K together with the corresponding spectra after subsequent annealing the matrix to 6 K and 9 K and relaxing it back to 3 K. It appears that the higher population of the A sub-level of the vibrational ground state at 2.8 K favors the two A–E and A–A transitions observed at
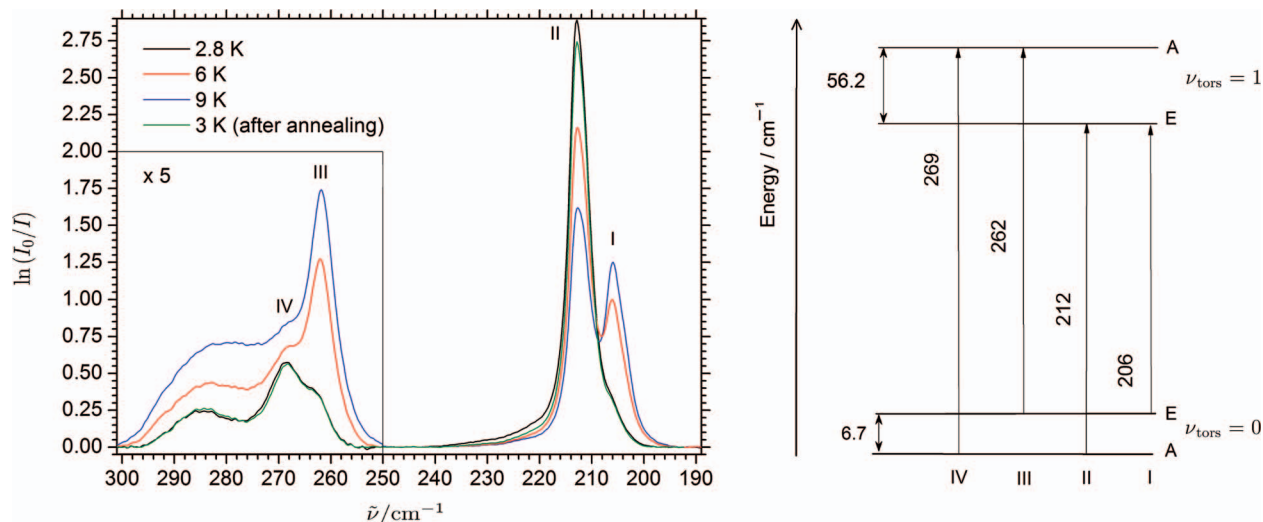
FIG. 3. The temperature dependence of the observed far-infrared absorption spectrum of methanol embedded in neon annealed from 2.8 K to 6 K and 9 K and relaxed back to 3 K (left). The assignments of the four different observed components I, II, III, and IV for the torsional fundamental ($v_{tors} = 0 \rightarrow 1$) of methanol monomer are indicated together with a corresponding torsional energy diagram illustrating the different A/E transitions (right).

212 cm^{-1} (denoted II) and 269 cm^{-1} (denoted IV), respectively. The slow, step-wise annealing reveals the emergence of the two torsional E–E and E–A transitions originating from the E sub-level of the vibrational ground state which gradually becomes more populated with increasing temperature. These bands, observed at 206 cm^{-1} (denoted I) and 262 cm^{-1} (denoted III), are red-shifted by the vibrational ground-state splitting of 6.7 cm^{-1} relative to the "cold" transitions (II and IV). In the matrix isolation spectra recorded at 2.8 K where the "cold" sub-bands dominate, another band is reproduced at 286 cm^{-1}. The concentration dependency of this band, although somewhat distorted by the overlap with the 269 cm^{-1} feature (IV), is steeper than observed for the four monomer sub-bands, which points at a dimer origin. This is supported by the blue-shifted position relative to the monomer band system and the fact that it collapses into a single band. The methanol:neon mixing ratios in the permille region rule out any methanol trimer assignments which is also supported by the lack of any corresponding trimer absorption in the OH stretching region (not shown).

Fig. 4 shows the entire far-infrared absorption spectrum of methanol embedded in neon at 2.8 K from 200 cm^{-1} up to the high-wavenumber cut-off of the cold optical filter inside the Si bolometer around 600 cm^{-1}. In the upper far-infrared region, a strong band is observed at 446 cm^{-1} even at the smallest methanol:neon mixing ratios, pointing at a monomer origin. This slightly broadened band has previously been observed by Perchard for very diluted methanol doped neon matrices.[47] At higher methanol:neon mixing ratios, another weak band appears at 507 cm^{-1} with the same concentration dependency. The intensity of these two bands also decreases by the same amount upon annealing of the neon matrices. A detailed assignment of these monomer transitions is difficult. However, we cannot reject Perchard's tentative assignment of the strong 446 cm^{-1} band to a torsional overtone transition originating from the A sub-level of the vibrational ground state.[47] In some matrix experiments, another

weak band with varying intensity is observed at 527 cm^{-1} in methanol-doped neon matrices. This band is attributed to water/methanol dimers which shall not be discussed further in the present contribution. At higher methanol:neon mixing ratios, a sharp band with one or more high-wavenumber shoulders appears at 558 cm^{-1}. This band has a steep concentration dependency which qualitatively matches the behavior of the broader proposed acceptor OH torsional mode at 286 cm^{-1}. As mentioned above, the latter band overlaps with the neighboring monomer feature which complicates a solid quantitative intensity analysis. Nevertheless, the two dimer bands in question appear to have almost the same integrated intensity at low methanol concentrations. This is supported by harmonic MP2 and B3LYP frequency calculations[5] which predict an almost 1:1 intensity ratio of these bands. These predictions

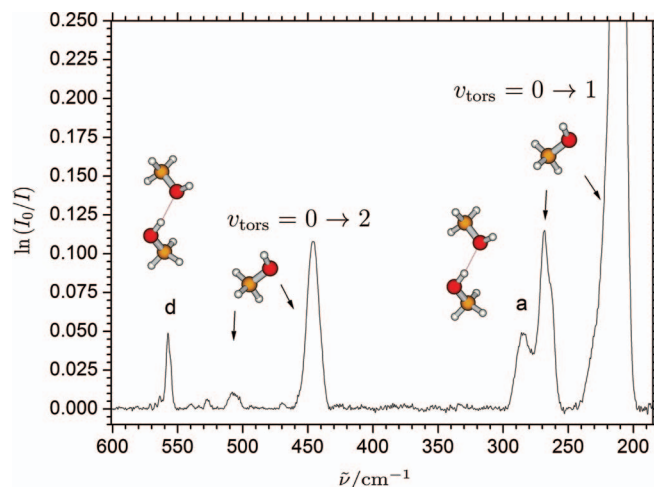FIG. 4. The observed far-infrared absorption spectra of methanol embedded in neon matrices at 2.8 K. The components of the torsional fundamental ($v_{tors} = 0 \rightarrow 1$) and first torsional overtone ($v_{tors} = 0 \rightarrow 2$) transitions of the monomer as well as of the acceptor OH torsional ("a") and donor OH librational ("d") transitions of the dimer are assigned by minimum structures.

suggest a straightforward assignment of the 558 cm^{-1} band to the missing donor OH librational band of methanol dimer.

The matrix band position lines up between the strong 551 cm^{-1} band and the weaker 567 cm^{-1} band observed in the jet spectra. A recent review article addressing water clusters embedded in neon matrices reports that large-amplitude intermolecular vibrational transitions tend to become slightly blue-shifted relative to the gas phase.[49] These small blue-shifts of large-amplitude vibrational modes are ascribed as minor repulsive steric effects originating from the neon host environment. This provides a qualitative argument in support for a dimer assignment of the 551 cm^{-1} band in the far-infrared jet spectrum. On the other hand, the predicted 1:1 intensity relationship mentioned above together with the lack of strong dimer absorptions at lower wavenumbers in the jet spectrum provide a counter-argument for an assignment of the weaker 567 cm^{-1} band to the librational mode in question. In the jet experiments, it is furthermore possible that the librational intensity is distributed over several $\Delta K = \pm 1$ sub-branches or affected by rovibrational couplings, similar to but less pronounced than in the case of the HF dimer.[50] In addition, the blue-shift observations cited above are not a strict indicator, since numerous red-shifts have been observed under similar conditions as well. Further, our previous quantum-chemical predictions[5] point at a possible overlap between the donor OH librational mode of the dimer and the lowest-wavenumber OH librational mode of the trimer. The far-infrared jet spectral series is thus less conclusive than the neon matrix isolation data, and we can only suggest a band origin interval of 560±10 cm^{-1} for the OH librational mode of the methanol dimer when not affected by a neon matrix environment.

In order to verify the proposed methanol dimer assignment further, we explore the isotopic spectral shifts associated with H/D substitution on the hydroxy group. Fig. 5 shows the full far-infrared absorption spectrum of methanol-OD embedded in neon at 2.8 K (red trace) together with the cor-
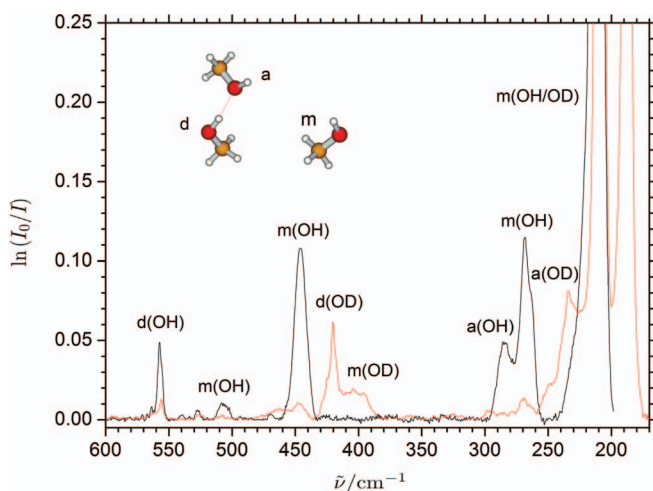
responding far-infrared spectrum of regular methanol (black trace) at a similar methanol:neon mixing ratio. H/D exchange processes on the very large surface of the matrix inlet tubing are inevitable, preventing higher purities than 80%–85% of methanol-OD in the deposited neon matrices. The traces of regular methanol can be monitored most clearly by the isolated torsional overtone sub-band observed at 447 cm^{-1}. The torsion-vibration splittings of the ground and excited torsional states are smaller for methanol-OD, owing to the slower torsional tunneling of D relative to H. Two major bands are reproduced at 187.5 cm^{-1} and 205.5 cm^{-1}; the latter being overlapped by the two torsional E–E and A–E sub-bands of regular methanol. These two bands have previously been observed by Perchard for very diluted methanol-OD doped neon matrices and assigned to the "cold" torsional sub-bands originating from the A sub-level of the vibrational ground state.[47] The two remaining torsional sub-bands originating from the E sub-level could not be observed by dedicated annealing experiments. The vibrational ground state splitting of methanol-OD in the gas phase is 2.6 cm^{-1} and might be even smaller in neon matrices.[51] The splitting of the excited torsional state of methanol-OD must therefore be very close to the wavenumber difference of ∼18 cm^{-1} between the "cold" torsional sub-bands.

In the regions of the proposed dimer assignments for regular methanol, we also observe small traces of deuterated dimeric species. A closer inspection of the region for the proposed donor OH librational band reveals a rather small red shift of ∼1–2 cm^{-1} relative to the band origin of 558 cm^{-1}. This small isotopic wavenumber shift points at a OH librational mode and could originate from mixed methanol dimers where regular methanol acts as a donor and methanol-OD acts as the acceptor. A red-shift of the same size is also observed for the mixed water/methanol dimer band around 527 cm^{-1} which shall not be discussed further in the present contribution. A series of previous cluster studies have shown that D-bonded complexes in general are more stable than the corresponding H-bonded complexes due to smaller zero-point energies.[52] Accordingly, the mixed methanol dimer where methanol-OD acts as the donor should be more abundant. In the region of the proposed acceptor OH torsional mode of the methanol dimer, we observe a rather weak and very broad spectral feature overlapped by the torsional E–A and A–A sub-bands of regular methanol. This broad spectral feature must have a contribution from mixed methanol dimers where regular methanol acts as acceptor instead of donor, but a quantitative analysis of the relative abundance of mixed methanol dimers is not possible even at higher mixing ratios.

The inevitable H/D exchange does not prevent a large excess of methanol-OD and clear absorption by the methanol-OD dimer. The donor OD librational mode is easily assigned as a rather sharp band at 420 cm^{-1}. The somewhat broad spectral feature observed below the sharp donor OD-librational band around 400 cm^{-1} appears to have a similar concentration dependency as the torsional sub-bands of methanol-OD and might originate from a monomeric torsional overtone sub-band. The acceptor OD torsional mode appears clearly as a high-wavenumber shoulder on the torsional A–A sub-band of methanol-OD at 234 cm^{-1}. This acceptor OD torsional

FIG. 5. The observed far-infrared absorption spectra of methanol (black trace) and methanol-OD (∼80%, red trace) embedded in neon matrices at 2.8 K. The assignments for the torsional fundamental and the first torsional overtone of the monomers (denoted "m(. . .)") as well as the acceptor OH/OD torsional (denoted "a") and donor OH/OD librational modes of the hydrogen-bonded methanol dimers (denoted "d") are shown (see text).

TABLE I. The observed band origins (in cm^{-1}) for the acceptor OH/OD torsional mode and the donor OH/OD librational mode of different hydrogen-bonded methanol dimer isotopologues isolated in supersonic jet expansions and embedded in cryogenic neon matrices at 2.8 K.

Species	Jet	Neon matrix
$(CH_3OH)_2$ acceptor OH torsion	Not assigned	286
$(CH_3OH)_2$ donor OH libration	560 ± 10	558
$(CH_3OD)_2$ acceptor OD torsion	Not assigned	234
$(CH_3OD)_2$ donor OD libration	Not assigned	420

band must be overlapped by mixed methanol dimers where methanol-OD acts as the acceptor and regular methanol as the donor which can explain the apparent larger band intensity relative to the acceptor OH torsional band of regular methanol dimer. The resulting OD/OH isotope ratios of 0.75–0.82 are significantly larger than $1/\sqrt{2}$ as expected for strongly anharmonic potential energy wells. The complete set of methanol dimer assignments from the combined jet and neon matrix isolation experiments is summarized in Table I.

V. HARMONIC LOCAL-CORRELATION COUPLED CLUSTER AND ANHARMONIC PREDICTIONS

Harmonic predictions for the donor OH stretching red-shift of the methanol dimer have been available for some time from MP2 and Density Functional Theory (DFT) calculations.[22] These predictions demonstrate a red-shift on the order of 150 cm^{-1}, much more than the experimental anharmonic value of 111 cm^{-1}. A recent study has now applied harmonic Coupled-Cluster methods in a local correlation framework (prefix L) to the problem,[23] providing a full normal-mode analysis at the optimized structures while being essentially free of basis set superposition error (BSSE). The exaggerated MP2 red-shifts were traced to an underestimation of the O–H bond strength of the donor molecule in the dimer, which is only partially compensated by likewise underestimated intermolecular electron correlation effects. A combination of local and explicit electron correlation beyond second-order perturbation theory placed the harmonic donor OH stretching red-shift close to 121 cm^{-1}.

Harmonic transition wavenumbers for the acceptor OH torsional and the donor OH librational modes were obtained at the same levels[23] and are reproduced in Table II. We augment these data with MP2/cc-pVTZ, B2PLYP-D3/cc-pVTZ, and B3LYP-D3BJ/6-311+G(2d,p) calculations making use of Grimme's empirical dispersion correction (D3)[53] and Becke-Johnson damping (BJ),[54] both in the harmonic approximation (Table II) and applying a standard second-order perturbational (VPT2) anharmonic treatment as implemented in the Gaussian 09 program,[29] carried out and reported in Ref. 24 and summarized in Table III. For brevity, we shorten the 6-311+G(2d,p) basis set to "6311" and cc-pVTZ to "VTZ." The VPT2 calculations avoided diffuse functions on all hydrogen atoms (6311) or even altogether (VTZ), improving numerical stability in the finite-displacement steps of the VPT2 treatment. The highest level of theory in Ref. 23 with an optimized geometry and harmonic frequencies is explicitly correlated

TABLE II. Harmonic wavenumbers ω (units of cm^{-1}) for the OH torsional ("tors") mode of the methanol monomer ("mon") and corresponding donor OH librational ("lib") and acceptor torsional ("tors") modes of the dimer ("dim"), reproduced from Refs. 24 and 23.

	ω_{tors}^{mon}	ω_{lib}^{dim}	ω_{tors}^{dim}
MP2/VTZ	309	699	317
B3LYP-D3BJ/6311	294	708	355
B2PLYP-D3/VTZ	304	694	308
MP2/A′VTZ[a]	294	695	331
LMP2/A′VTZ	293	660	319
LCCSD(T0)/A′VTZ(int)	294	647	320
Benchmark[b]	294	660	322

[a]Diffuse functions omitted for CH_3 hydrogens.
[b]LCCSD(T*)-F12a/VDZ-F12(int).

LCCSD(T)-F12/cc-pVDZ-F12(int), with the intermolecular interactions ("int") treated at the same high level of theory. Comparison with larger basis sets showed that these results were very close to the Complete Basis Set (CBS) limit. We can therefore regard these data as the harmonic benchmark for all other calculations henceforth.

The harmonic OH librational wavenumbers are overestimated in the canonical MP2 and DFT calculations by 30–50 cm^{-1}. This correlates with overestimated OH stretching shifts, indicative of a too anisotropic hydrogen bond. The good performance of LMP2 is a result of error compensation and does not extend to the OH stretching shift.[23]

Advancing to the anharmonic VPT2 results which are restricted to lower electronic structure levels (Table III), the donor OH librational mode exhibits a pronounced negative diagonal anharmonicity, red-shifting the fundamental transition by about 90 cm^{-1}. This corresponds to a sub-linear increase of the restoring force due to the directional hydrogen bond. The off-diagonal couplings to all other modes are predicted to slightly increase this red-shift when taken together, but a distinct positive coupling to the donor OH stretching vibration can be identified. This coupling reflects the fact that

TABLE III. Calculated VPT2 spectroscopic constants (units of cm^{-1}) for the donor OH librational mode of methanol dimer (from Ref. 24 and by personal communication of the computer outputs through its authors). The 20 anharmonic coupling cross-terms not given in the table are somewhat smaller and their overall sum is very close to 0.

	MP2/VTZ	B3LYP-D3BJ/6311	B2PLYP-D3/VTZ
ω_{lib} [a]	699	708	694
$2x_{lib,\,lib}$ [b]	-92	-91	-85
$\frac{1}{2}x_{lib,\,\nu(OH)_b}$ [c]	$+30$	$+30$	$+30$
$\frac{1}{2}x_{lib,\,\delta(OH)_b}$ [d]	-9	-8	-8
$\frac{1}{2}x_{lib,\,tors}$ [e]	-7	-11	-7
$\frac{1}{2}\sum_1^6 x_{lib,\,intermol}$ [f]	-31	-31	-21
$\tilde{\nu}_{lib}$ [g]	589	595	603

[a]The harmonic wavenumber.
[b]The anharmonic contribution from diagonal anharmonicity.
[c]The anharmonic contribution from the coupling to the donor OH stretching mode.
[d]The anharmonic contribution from the coupling to the donor OH bending mode.
[e]The anharmonic contribution from the coupling to the acceptor OH torsional mode.
[f]The anharmonic contribution from the coupling to the six intermolecular modes.
[g]The anharmonic wavenumber.

TABLE IV. Calculated VPT2 spectroscopic constants (units of cm^{-1}) for the acceptor OH torsional mode of methanol dimer (from Ref. 24 and by personal communication of the computer outputs through its authors).

	MP2/VTZ	B3LYP-D3BJ/6311	B2PLYP-D3/VTZ
ω_{tors} [a]	317	355	308
$2x_{tors, tors}$ [b]	−66	−61	−73
$\frac{1}{2}\sum_{j}^{29} x_{tors,j}$ [c]	+31	−9	+11
$\tilde{\nu}_{tors}$ [d]	282	285	246

[a]The harmonic wavenumber.
[b]The anharmonic contribution from diagonal anharmonicity.
[c]The anharmonic contribution from the sum of all coupling cross-terms to the other 29 vibrational modes.
[d]The anharmonic wavenumber.

the OH librational mode is ultimately of dissociative nature, and its excitation tends to restore the higher monomer value for the OH stretching frequency. The magnitude of this coupling is remarkably consistent among the calculations, independent of variations in the absolute harmonic wavenumbers for the OH librational and stretching modes. The positive $x_{lib,\nu(OH)_b}$ coupling is key responsible for the fact that the harmonic OH stretching red-shift of methanol dimer is larger than the experimental one despite opposing diagonal anharmonic OH stretching effects. Indeed, from the experimental constraints outlined in the Introduction,[23, 24] one can estimate the order of magnitude of $\frac{1}{2}x_{lib,\nu(OH)_b}$ around 36 cm^{-1}, if all other off-diagonal contributions to the OH stretching shift are assumed to approximately cancel. All this lends some credibility to the VPT2 corrections despite their limited electronic structure level and the relatively large amplitude motion in the OH librational mode, which probably challenges the applicability of the VPT2 approximations.

The overall sum of anharmonic corrections to the librational fundamental transition is on the order of $-(100 \pm 10)$ cm^{-1}. Adding this to the benchmark harmonic wavenumber of 660 cm^{-1}, a prediction of 560 cm^{-1} is obtained which is fully consistent with the present experimental value of (560 ± 10) cm^{-1}. A similar analysis of the acceptor OH torsional mode of methanol dimer is likely to stretch the reliability of VPT2 calculations, but we note that the best harmonic estimate of 322 cm^{-1} (Table II) in combination with the average VPT2 correction of (50 ± 20) cm^{-1} (Table IV) is not too far from the experimental value of 286 cm^{-1} obtained in this work.

We finally note that the overtone of the hydrogen-bonded librational mode is predicted remarkably close to the CO stretching fundamentals of methanol dimer[13] based on the results of the present work, potentially complicating their quantitative analysis.

VI. CONCLUSIONS

For the first time, the fundamental hydrogen bond librational mode of the smallest organic hydrogen-bonded dimer has been confidently assigned experimentally near 560 cm^{-1} with an accuracy which allows for rigorous benchmarking of theory. The remaining experimental uncertainty of at most

± 10 cm^{-1} is due to spectral overlap with methanol trimer (in the gas phase) or residual matrix influence (in the cryogenic neon matrix). The 100 cm^{-1} or 15% gap to the benchmark harmonic prediction can be rationalized mostly by anharmonicity along the librational coordinate. Off-diagonal coupling terms are significant, in particular to the bound OH stretching mode, but they are largely canceled by opposing coupling cross-terms from the intermolecular modes. The experimental result is corroborated by results for O-deuterated methanol dimer (420 cm^{-1}) and the even larger amplitude acceptor OH (OD) torsional mode of the dimer is observed at 286 cm^{-1} (234 cm^{-1}) in the neon matrices. Thus, two orthogonal degrees of freedom of the hydrogen bonded (and free) OH groups in methanol dimer as well as their mutual coupling are now rather well established by infrared vibrational spectroscopy. Sensitivity limits of supersonic jet spectroscopy in the far infrared and environmental effects in neon matrices are seen to be surmountable by a combination of both techniques. Quantitative studies of sub-picosecond intermolecular energy flow in organic hydrogen bonds can profit from these reference values. It would be valuable to confirm some of the conclusions on off-diagonal coupling cross-terms by direct observation of weak OH stretching-libration combination bands of methanol dimer.

[1]P. Maksyutenko, O. Boyarkin, T. Rizzo, and D. Perry, J. Chem. Phys. **126**, 044311 (2007).
[2]R. M. Lees, L.-H. Xu, J. W. C. Johns, B. P. Winnewisser, and M. Lock, J. Mol. Spectrosc. **243**, 168–181 (2007).
[3]D. J. Nesbitt, J. Phys. Chem. **100**, 12735–12756 (1996).
[4]A. D. Mackerell, Jr., J. Comput. Chem. **25**, 1584–1604 (2004).
[5]R. Wugt Larsen and M. A. Suhm, J. Chem. Phys. **125**, 154314 (2006).
[6]R. Wugt Larsen and M. A. Suhm, Phys. Chem. Chem. Phys. **12**, 8152–8157 (2010).
[7]T. Yagasaki, J. Ono, and S. Saito, J. Chem. Phys. **131**, 164511 (2009).
[8]R. Jiang and E. L. Sibert, J. Phys. Chem. A **113**, 7275–7285 (2009).
[9]R. Jiang and E. L. Sibert, J. Chem. Phys. **136**, 224104 (2012).
[10]C. L. Lugez, F. J. Lovas, J. T. Hougen, and N. Ohashi, J. Mol. Spectrosc. **194**, 95–112 (1999).
[11]F. J. Lovas, S. P. Belov, M. Y. Tretyakov, W. Stahl, and R. Suenram, J. Mol. Spectrosc. **170**, 478–492 (1995).
[12]M. A. Hoffbauer, C. F. Giese, and W. R. Gentry, J. Phys. Chem. **88**, 181–184 (1984).
[13]F. Huisken and M. Stemmler, Chem. Phys. Lett. **144**, 391–395 (1988).
[14]U. Buck, X. J. Gu, C. Lauenstein, and J. Rudolph, J. Chem. Phys. **92**, 6017 (1990).
[15]J. P. La Cosse and J. M. Lisy, J. Phys. Chem. **94**, 4398–4400 (1990).
[16]A. Bizzarri, S. Stolte, J. Reuss, J. Van Duijneveldt-van De Rijdt, and F. Van Duijneveldt, Chem. Phys. **143**, 423–435 (1990).
[17]U. Buck and F. Huisken, Chem. Rev. **100**, 3863–3890 (2000).
[18]F. Huisken and A. Kulcke, J. Chem. Phys. **95**, 3924–3929 (1991).
[19]R. A. Provencal, J. B. Paul, K. Roth, C. Chapo, R. N. Casaes, R. J. Saykally, G. S. Tschumper, and H. F. Schaefer III, J. Chem. Phys. **110**, 4258–4267 (1999).

[20] H. Han, C. Camacho, H. Witek, and Y.-P. Lee, J. Chem. Phys. **134**, 144309 (2011).

[21] T. Häber, U. Schmitt, and M. A. Suhm, Phys. Chem. Chem. Phys. **1**, 5573–5582 (1999).

[22] R. Wugt Larsen, P. Zielke, and M. A. Suhm, J. Chem. Phys. **126**, 194307 (2007).

[23] M. Heger, M. A. Suhm, and R. A. Mata, J. Chem. Phys. **141**(10), 101105 (2014); Supplementary material is available at ftp://ftp.aip.org/epaps/journ_chem_phys/E-JCPSA6-141-034436.

[24] F. Kollipost, K. Papendorf, Y.-F. Lee, Y.-P. Lee, and M. A. Suhm, Phys. Chem. Chem. Phys. **16**, 15948–15956 (2014); Supplementary material is available at http://pubs.rsc.org/en/Content/ArticleLanding/2014/CP/c4cp01418a.

[25] J. Murto, M. Räsänen, A. Aspiala, and E. Kemppinen, Acta Chem. Scand. A **37a**, 323–335 (1983).

[26] S. Coussan, Y. Bouteiller, A. Loutellier, J. P. Perchard, S. Racine, A. Peremans, W. Q. Zheng, and A. Tadjeddine, Chem. Phys. **219**, 221–234 (1997).

[27] S. Coussan, A. Loutellier, J. P. Perchard, S. Racine, A. Peremans, A. Tadjeddine, and W. Q. Zheng, Chem. Phys. **223**, 279–292 (1997).

[28] J. P. Perchard and Z. Mielke, Chem. Phys. **264**, 221–234 (2001).

[29] V. Barone, J. Chem. Phys. **122**(1), 014108 (2005).

[30] I. M. Mills, *Vibration-rotation Structure in Asymmetric- and Symmetric-top Molecules in Molecular Spectroscopy: Modern Research*, edited by N. Rao and C. W. Mathews (Academic, 1972), Vol. I, pp. 115–140.

[31] G. Amat, H. Nielsen, and G. Tarrago, *Rotation-vibration Spectra of Molecules* (Marcel Dekker, New York, 1971).

[32] M. A. Suhm and F. Kollipost, Phys. Chem. Chem. Phys. **15**, 10702–10721 (2013).

[33] J. Andersen, J. Heimdal, D. W. Mahler, B. Nelander, and R. Wugt Larsen, J. Chem. Phys. **140**, 091103 (2014).

[34] A. Serrallach, R. Meyer, and H. H. Günthard, J. Mol. Spectrosc. **52**, 94–129 (1974).

[35] J. R. Dixon, W. O. George, F. Hossain, R. Lewis, and J. M. Price, J. Chem. Soc., Faraday Trans. **93**, 3611–3618 (1997).

[36] F. Huisken, M. Kaloudis, M. Koch, and O. Werhahn, J. Chem. Phys. **105**, 8965–8968 (1996).

[37] U. Buck, J.-G. Siebers, and R. J. Wheatley, J. Chem. Phys. **108**, 20–32 (1998).

[38] Y. Liu, M. Weimann, and M. A. Suhm, Phys. Chem. Chem. Phys. **6**, 3315–3319 (2004).

[39] P. Zielke and M. A. Suhm, Phys. Chem. Chem. Phys. **8**, 2826–2830 (2006).

[40] R. H. Hunt, W. N. Shelton, F. A. Flaherty, and W. B. Cook, J. Mol. Spectrosc. **192**, 277–293 (1998).

[41] B. Fehrensen, D. Luckhaus, M. Quack, M. Willeke, and T. R. Rizzo, J. Chem. Phys. **119**, 5534–5544 (2003).

[42] G. Moruzzi, M. Winnewisser, B. P. Winnewisser, I. Mukhopadhyay, and F. Strumia, *Microwave, Infrared, and Laser Transitions of Methanol Atlas of Assigned Lines from 0 to 1258 cm^{-1}* (CRC Press, Inc., 1995).

[43] D. G. Burkhard and D. M. Dennison, J. Mol. Spectrosc. **3**, 299 (1959).

[44] M. Hepp, I. Pak, K. Yamada, E. Herbst, and G. Winnewisser, J. Mol. Spectrosc. **166**, 66–78 (1994).

[45] F. Kollipost, R. Wugt Larsen, A. V. Domanskaya, M. Noerenberg, and M. A. Suhm, J. Chem. Phys. **136**, 151101 (2012).

[46] Y.-P. Lee, Y.-J. Wu, R. M. Lees, L.-H. Xu, and J. T. Hougen, Science **311**, 365–368 (2006).

[47] J. P. Perchard, Chem. Phys. **332**, 86–94 (2007).

[48] J. P. Perchard, F. Romain, and Y. Bouteiller, Chem. Phys. **343**, 35–46 (2008).

[49] J. Ceponkus, A. Engdahl, P. Uvdal, and B. Nelander, Chem. Phys. Lett. **581**, 1–9 (2013).

[50] M. Quack and M. A. Suhm, Theor. Chim. Acta **93**, 61–65 (1996).

[51] I. Mukhopadhyay, Spectrochim. Acta **54**, 1325 (1998).

[52] A. Engdahl and B. Nelander, J. Chem. Phys. **86**, 1819 (1987).

[53] S. Grimme, J. Antony, S. Ehrlich, and H. Krieg, J. Chem. Phys. **132**, 154104 (2010).

[54] S. Grimme, S. Ehrlich, and L. Goerigk, J. Comput. Chem. **32**, 1456–1465 (2011).